Hindawi
Advances in High Energy Physics
Volume 2021, Article ID 9991152, 7 pages
https://doi.org/10.1155/2021/9991152

Research Article

Charmonium Properties Using the Discrete Variable Representation (DVR) Method

Bhaghyesh A.

Department of Physics, Manipal Institute of Technology, Manipal Academy of Higher Education, 576104, Manipal, India

Correspondence should be addressed to Bhaghyesh A.; bhaghyesh.mit@manipal.edu

Received 19 March 2021; Accepted 16 July 2021; Published 30 July 2021

Academic Editor: Shi Hai Dong

The Schrödinger equation is solved numerically for charmonium using the discrete variable representation (DVR) method. The Hamiltonian matrix is constructed and diagonalized to obtain the eigenvalues and eigenfunctions. Using these eigenvalues and eigenfunctions, spectra and various decay widths are calculated. The obtained results are in good agreement with other numerical methods and with experiments.

1. Introduction

The first quarkonium state was discovered independently at SLAC [1] and BNL [2], confirming the existence of heavy quark bound states. Since then, quarkonium has always been of great interest to particle physicists, being one of the extensively investigated system both theoretically and experimentally [3, 4]. New states are continuously being detected at various experiments. Recently, the LHCb collaboration [5] has detected a new state $X(3842)$ which is interpreted as a candidate for the unobserved $\psi_3(1^3D_3)$ state. Both charmonium and bottomonium have rich spectrum of states below the open flavor threshold which have been experimentally observed, and various decay widths of these states have also been measured [6]. Studies on heavy quark systems are important because it gives information about quark interaction potential, confinement, QCD coupling constant, CKM matrix elements, and various other inputs to the standard model, some of which cannot be directly obtained from QCD.

Theoretically, quarkonium systems have been studied by various formalisms based on phenomenological potential models [7–11], effective field theory [12], lattice gauge theory [13–16], Bethe Salpeter equation [17–20], etc. Among these, owing to its simplicity, formalism based on potential models is the widely chosen method to investigate quarkonium systems. In this method, both relativistic and quantum corrections can be easily incorporated. Potential models have been highly successful in predicting the spectra and decay widths [7, 9, 10]. In potential models, the usual method is to extract the properties of quarkonium by solving the Schrödinger equation using a chosen quark-antiquark potential. The widely used quark-antiquark potential in phenomenological models is the so-called Cornell potential [21–25], which includes a short-range Coulomb term and a linear confinement term. The form of this potential is also confirmed by lattice QCD calculations [26, 27].

The Schrödinger equation for most of the $q\bar{q}$ potentials (including the Cornell potential) cannot be solved analytically; hence, numerical solutions are called for. Some of the methods found in literature for solving the Schrödinger equation for $q\bar{q}$ systems are numerical methods based on Runge-Kutte approximation [28, 29], Numerov matrix method [30–32], asymptotic iteration method [33–35], Fourier grid Hamiltonian method [36], variational method [37, 38], etc. Another method for numerically solving the Schrödinger equation is the discrete variable representation (DVR) method. This method has not been applied to quarkonium spectroscopy. Hence, in this article, we numerically solve the Schrödinger equation for $c\bar{c}$ system using the discrete variable representation (DVR) scheme of Colbert and Miller [39]. DVR method was initially introduced by Harris

et al. [40] and was extensively developed by Light and coworkers [41–46]. DVRs provide highly efficient and accurate solutions to quantum dynamical problems and have been widely used in atomic physics and quantum chemistry [47–56]. More details on DVR methods can be found in refs. [57, 58].

This paper is organised as follows: a brief discussion on the potential model used to describe the $c\bar{c}$ system and the DVR scheme used to solve the Schrödinger equation are presented in Section 2. The various decay properties calculated in the present analysis are given in Section 3. Results and discussions of the present work are given in Section 4.

2. Formalism

As a minimal model describing charmonium, we have used a nonrelativistic potential model, with the Hamiltonian

$$H = M + \frac{p^2}{2\mu} + V(r), \tag{1}$$

where p is the relative momentum, $\mu(= m_c m_{\bar{c}}/m_c + m_{\bar{c}})$ is the reduced mass of the $c\bar{c}$ system, $M = m_c + m_{\bar{c}}$, and $V(r)$ is the quark-antiquark potential. m_c and $m_{\bar{c}}$ are the masses of individual quark and antiquark, respectively. For describing the quark-antiquark interaction, we use the standard Cornell potential plus a Gaussian-smeared contact hyperfine interaction [7]:

$$V(r) = -\frac{4}{3}\frac{\alpha_c}{r} + br + V_0 + \frac{32\pi\alpha_c}{9m_c^2}\left(\frac{\sigma}{\sqrt{\pi}}\right)^3 e^{-\sigma^2 r^2}\vec{S}_c \cdot \vec{S}_{\bar{c}}. \tag{2}$$

Parameters used in eq. (2) are given in Table 1 and are obtained by fitting the spectrum. Charmonium properties can be obtained by solving the Schrödinger equation corresponding to the Hamiltonian given in eq. (1) with potential given in eq. (2). In this work, to solve the Schrödinger equation, we have used the DVR scheme of Colbert and Miller [39]. In the DVR, the Hamiltonian is represented by a matrix on a uniform grid of points ($r_i = i\Delta r$, $i = 1, 2, 3, ..$) in the coordinate space. Once the H-matrix is constructed, diagonalization gives us the bound state eigenvalues and the amplitudes of eigenfunctions on the grid point chosen.

In ref. [39], authors have shown that the kinetic energy matrix can be written as

$$T_{ij} = \frac{\hbar^2}{2m\Delta r^2}(-1)^{i-j}\begin{cases} \dfrac{\pi^2}{3} - \dfrac{1}{2i^2} & i = j, \\ \dfrac{2}{(i-j)^2} - \dfrac{2}{(i+j)^2} & i \neq j, \end{cases} \tag{3}$$

with $r_i = i\Delta r$, $(i = 1, 2, \cdots)$, where Δr is the grid spacing. The potential energy matrix is diagonal

$$V_{ij} = V(r_i)\delta_{ij}. \tag{4}$$

We have used eqs. (1)–(4) to construct the Hamiltonian matrix in the present model, which upon diagonalization returns the bound state eigenvalues and the amplitudes of eigenfunctions on the chosen grid points. In the present analysis, we have chosen a grid of length 10 fm with 1000 grid points. The eigenvalue problem for the matrix of the Hamiltonian (1) was solved using Mathematica. For a given eigenvalue, in order to obtain the eigenfunction in the entire range of coordinates, we have used the built-in interpolation function in Mathematica through the obtained eigenfunctions on grid points. This interpolation function was used as the representation of the reduced radial wavefunction for our further analysis. Obtained wavefunctions for $^3S_1$ and ^3P_J states are shown in Figure 1. In order to compute fine structure of the $L \neq 0$ states, we add the spin-orbit and tensor terms perturbatively [7]:

$$V_{fs} = \frac{1}{m_c^2}\left[\left(\frac{2\alpha_c}{r^3} - \frac{b}{2r}\right)\vec{L}\cdot\vec{S} + \frac{4\alpha_c}{r^3}T\right]. \tag{5}$$

The computed mass spectra of charmonium are listed in Table 2. Using the obtained wavefunction, we also compute the root mean square radii ($\sqrt{<r^2>}$) and the square of the radial wavefunction at the origin ($|R(0)|^2$) for these states, and our results are listed in Table 3.

Table 1: Parameters used in the model.

Parameter	Value
α_c	0.54
b	0.136 GeV^2
V_0	0.149 GeV
σ	1.1 GeV
m_c	1.4 GeV

3. Decay Properties

For quarkonium, most of the decay properties are dependent on the wave function. Hence, to test the wavefunctions as obtained in the previous section, we calculate leptonic decay widths and radiative decay widths ($M1$ and $E1$) of some charmonium states.

3.1. Leptonic Decay Widths. The leptonic decay widths of the vector states are calculated using the Van Royen-Weisskopf formula [63, 64].

$$\Gamma_{ee} = \frac{4\alpha^2 e_c^2}{M_{nS}}|R_{nS}(0)|^2\left(1 - \frac{16\alpha_s}{3\pi}\right), \tag{6}$$

where M_{nS} is the mass for nS state, e_c is the charm quark charge in unit of electron charge, α is the fine structure constant, $\alpha_s \approx \alpha_s(2m_c)$ is the strong coupling constant, and $R_{ns}(0)$ is the radial nS wave function at the origin. The terms in parenthesis are the QCD radiative correction factor. Obtained results are listed in Table 4.

3.2. M1 Radiative Transitions. Magnetic dipole ($M1$) radiative transitions obey the selection rule $\Delta L = 0$ and $\Delta S = \pm 1$.

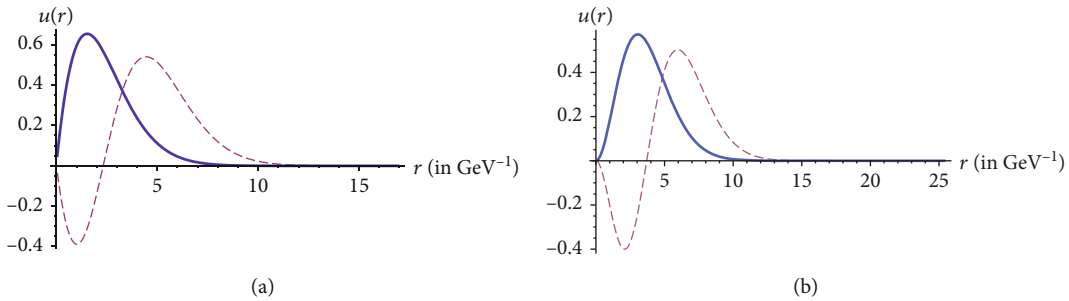

FIGURE 1: The wavefunctions of charmonium $^3S_1$ states (a) and ^3P_J states (b). Solid curve represents the $n = 1$ state while dashed curve represents the $n = 2$ state.

TABLE 2: Mass spectrum of charmonium states (in MeV).

State	Present	Exp [6]	[7]	[10]	[59]	[60]	[61]	[62]
J/ψ	3097	3096.900 ± 0.006	3090	3097	3094	3094	3090.0	3091.7
$\eta_c(1S)$	2986	2983.9 ± 0.5	2982	2979	2995	2989	2981.6	2992.4
$\psi(2S)$	3663	3686.097 ± 0.025	3672	3673	3649	3681	3671.8	3671.4
$\eta_c(2S)$	3620	3637.6 ± 1.2	3630	3623	3606	3602	3630.3	3631.7
$\psi(3S)$	4055	4039 ± 1	4072	4022	4036	4129	4071.6	4075.5
$\eta_c(3S)$	4025		4043	3991	4000	4058	4043.2	4048.1
$\psi(4S)$	4385	4421 ± 4	4406	4273	4362	4514	4406.1	4415.0
$\eta_c(4S)$	4360		4384	4250	4328	4448	4383.7	4393.3
$\psi(5S)$	4678			4463	4654	4863	4703.8	
$\eta_c(5S)$	4657			4446	4622	4799	4685.0	
$\psi(6S)$	4947			4608	4925	5185	4976.9	
$\eta_c(6S)$	4929			4595	4893	5124	4960.4	
$\chi_{c2}(1P)$	3546	3556.17 ± 0.07	3556	3554	3556	3480	3549.0	3548.1
$\chi_{c1}(1P)$	3498	3510.67 ± 0.05	3505	3510	3523	3468	3505.4	3501.8
$\chi_{c0}(1P)$	3419	3414.71 ± 0.30	3424	3433	3457	3428	3424.5	3425.8
$h_c(1P)$	3507	3525.38 ± 0.11	3516	3519	3534	3470	3515.6	3510.5
$\chi_{c2}(2P)$	3955		3972	3937	3956	3955	3964.8	3970.0
$\chi_{c1}(2P)$	3909		3925	3901	3925	3938	3924.9	3925.8
$\chi_{c0}(2P)$	3839		3852	3842	3866	3897	3852.3	3856.7
$h_c(2P)$	3918		3934	3908	3936	3943	3933.6	3933.4
$\psi_3(1^3D_3)$	3791		3806	3799	3801	3755	3805.3	3800.6
$\psi_2(1^3D_2)$	3786		3800	3798	3805	3772	3800.4	3796.7
$\psi(1^3D_1)$	3771	3773.13 ± 0.35	3785	3787	3799	3775	3785.0	3783.1
$\eta_{c2}(1^1D_2)$	3785		3799	3796	3802	3765	3799.4	3795.1
$\psi_3(2^3D_3)$	4146		4167	4103	4151	4176	4165.5	4167.1
$\psi_2(2^3D_2)$	4138		4158	4100	4152	4188	4158.2	4160.2
$\psi(2^3D_1)$	4122	4191 ± 5	4142	4089	4145	4188	4141.5	4145.1
$\eta_{c2}(2^1D_2)$	4138		4158	4099	4150	4182	4157.6	4159.1

Table 3: Average radii (in fm) and square of the radial wave function at the origin (in GeV^3).

State	$\sqrt{<r^2>}$	[62]	[61]	[10]	$\lvert R(0)\rvert^2$	[62]	[61]
$\eta_c(1S)$	0.380	0.375	0.3655		1.649	1.5405	1.2294
$\eta_c(2S)$	0.863	0.839	0.8328		0.731	0.7541	0.8717
$\eta_c(3S)$	1.250	1.210	1.2072		0.573	0.6088	0.683
$\eta_c(4S)$	1.584	1.531	1.5306		0.502	0.5430	0.5994
$\eta_c(5S)$	1.885		1.8225		0.461		0.5503
J/ψ	0.434	0.421	0.4143	0.41	0.976	1.1861	1.97675
$\psi(2S)$	0.897	0.867	0.8627	0.91	0.897	0.7092	0.7225
$\psi(3S)$	1.274	1.230	1.2287	1.38	1.274	0.5914	0.6006
$\psi(4S)$	1.603	1.547	1.5478	1.87	1.603	0.5340	0.5417
$\psi(5S)$	1.902		1.8370	2.39	1.902		0.50538
1^1P	0.700	0.678	0.6738		≈0	0	≈0
1^3P	0.712	0.689	0.7173	0.71	≈0	0	≈0
2^1P	1.108	1.071	1.0697		≈0	0	≈0
2^3P	1.120	1.082	1.1107	1.19	≈0	0	≈0
1^1D	0.931	0.899	0.8984		≈0	0	≈0
1^3D	0.932	0.901	0.9179	0.96	≈0	0	≈0
2^1D	1.304	1.258	1.2595		≈0	0	≈0
2^3D	1.305	1.261	1.1914	1.44	≈0	0	≈0

Table 4: Leptonic decay widths (in keV).

State	Present	Exp [6]	[59]	[60]	[65]	[10]
J/ψ	4.979	$5.55 \pm 0.14 \pm 0.02$	3.623	2.925	1.8532	6.60
$\psi(2S)$	2.137	2.33 ± 0.04	1.085	1.533	0.5983	2.40
$\psi(3S)$	1.460	0.86 ± 0.07	0.748	1.091	0.3812	1.42
$\psi(4S)$	1.131	0.58 ± 0.07	0.599	0.856	0.2847	0.97
$\psi(5S)$	0.930		0.508	0.707	0.2286	0.70

Table 5: $M1$ radiative partial widths (in keV).

Transition	Present	Exp [6]	[7]	[60]	[59]	[66]
$1\,^3S_1 \longrightarrow 1\,^1S_0$	2.66	1.58 ± 0.37	2.9	2.722	1.647	2.39
$2\,^3S_1 \longrightarrow 2\,^1S_0$	0.17	0.21 ± 0.15	0.21	1.172	0.135	0.19
$2\,^3S_1 \longrightarrow 1\,^1S_0$	5.02	1.00 ± 0.15	4.6	7.506	69.57	7.80

The $M1$ widths are evaluated using the formula [7].

$$\Gamma_{M1}\left(n^{2S+1}L_J \longrightarrow n'^{2S'+1}L'_{J'}\right) = \frac{4}{3}\frac{2J'+1}{2L+1}\delta_{LL'}\delta_{S,S'+1}e_c^2\frac{\alpha}{m_c^2} \cdot \left|<\psi_f \mid \psi_i>\right|^2 E_\gamma^3 \frac{E_f}{M_i}, \quad (7)$$

where E_γ is the emitted photon energy, $<\psi_f \mid \psi_i>$ is the overlap integral involving initial and final radial wavefunctions, E_f is the total energy of the final state, and M_i is the mass of the initial state. Calculated $M1$ widths are listed in Table 5.

3.3. E1 Radiative Transitions. Electric dipole ($E1$) radiative transitions obey the selection rule $\Delta L = \pm 1$ and $\Delta S = 0$. The

Table 6: $E1$ radiative partial widths (in keV).

Transition	Present	Exp [6]	[7]	[60]	[59]	[66]	[10]
$2\,^3S_1 \longrightarrow 1\,^3P_2$	29.78	27.99 ± 0.96	38	62.312	7.07	36	43
$2\,^3S_1 \longrightarrow 1\,^3P_1$	49.31	28.67 ± 1.05	54	43.292	10.39	45	62
$2\,^3S_1 \longrightarrow 1\,^3P_0$	49.38	28.78 ± 0.98	63	21.863	11.93	27	74
$1\,^3P_2 \longrightarrow 1\,^3S_1$	436.45	374.30 ± 19.73	424	157.225	233.85	327	473
$1\,^3P_1 \longrightarrow 1\,^3S_1$	319.08	288.12 ± 16.09	314	146.317	189.86	269	354
$1\,^3P_0 \longrightarrow 1\,^3S_1$	175.78	151.2 ± 9.99	152	112.030	118.29	141	167
$2\,^3D_1 \longrightarrow 1\,^3P_2$	6.07	<17.4	4.9	5.722	6.45	5.4	5.8
$2\,^3D_1 \longrightarrow 1\,^3P_1$	159.05	67.73 ± 6.73	125	93.775	139.52	115	150
$2\,^3D_1 \longrightarrow 1\,^3P_0$	425.59	187.68 ± 17.72	403	161.504	343.87	243	486

$E1$ widths are evaluated using the formula [7].

$$\Gamma_{E1}\left(n^{2S+1}L_J \longrightarrow n'^{2S'+1}L'_{J'}\right) = \frac{4}{3}C_{fi}\delta_{SS'}e_c^2\alpha\left|<\psi_f|r|\psi_i>\right|^2 E_\gamma^3\frac{E_f}{M_i}, \tag{8}$$

where $<\psi_f|r|\psi_i>$ is the spatial matrix element involving the initial and final radial wavefunctions, and C_{fi} is the angular matrix element given by

$$C_{fi} = \max\left(L, L'\right)\left(2J'+1\right)\begin{Bmatrix} L' & J' & S \\ J & L & 1 \end{Bmatrix}^2. \tag{9}$$

$E1$ widths obtained from the present analysis are listed in Table 6.

4. Discussion and Summary

In the present work, we have numerically solved the Schrödinger equation for charmonium system using the DVR scheme of Colbert and Miller. The Hamiltonian matrix was constructed and diagonalised to obtain the masses and wavefunctions of charmonium states. In Table 2, we compare the masses of radially and orbitally excited $c\bar{c}$ states with experiment [6] and other theoretical predictions [7, 10, 59–62]. Authors in refs. [7, 59–62] have also used Cornell type potential to study the $c\bar{c}$ system, where as in ref. [10], authors use a screened potential. From Table 2, we see that the predictions using the DVR method are in good agreement with experiment and other theoretical predictions. In Table 3, we have compared our predictions for the root mean square radii ($\sqrt{<r^2>}$) and the square of the radial wavefunction at the origin ($|R(0)|^2$) with other theoretical predictions [10, 61, 62]. The values of radial wavefunctions at the origin are important inputs for calculating quarkonium production cross-sections [22] and various decay amplitudes. We present our results for leptonic decays in Table 4 in comparison with experiment and other models. Our predictions for lower states are in good agreement with the experimental results. For higher excited states, our predictions are higher than the experimental results. We present results of $E1$ and $M1$ radiative transitions in Tables 5 and 6, respectively. Radiative transitions in quarkonia are important because they are one of the few mechanisms that produce transitions among $q\bar{q}$ states with different quantum numbers. This decay mechanism also helps to produce excited P-wave states and F-wave states which are otherwise difficult to achieve [7]. $M1$ decays in particular allow to access spin-singlet states. From Tables 5 and 6, we see that there is a wide range of precautions for the radiative decay widths even though all these models [7, 59, 60, 66] employ a Cornell type potential. This may be due to the difference in wavefunctions of charmonium states used in these models. Our predictions for radiative decays are in accordance with experiment and other theoretical predictions. Inclusion of higher multipole contributions, coupled channel effects, relativistic corrections, etc., would give a better fit to the experimental results.

In summary, in this article, we have successfully employed the DVR method to investigate the spectra and decays of charmonium. The obtained results of the present study are in good agreement with experimental data and with other theoretical models.

Data Availability

The data used to support the findings of this study are included within the article and are cited at relevant places within the text as references.

Conflicts of Interest

The author declares that he has no conflicts of interest.

References

[1] J. E. Augustin, A. M. Boyarski, M. Breidenbach et al., "Discovery of a narrow resonance in e^+e^- annihilation," *Physical Review Letters*, vol. 33, pp. 1406–1408, 1974.

[2] J. J. Aubert, U. Becker, P. J. Biggs et al., "Experimental observation of a heavy particle j," *Physical Review Letters*, vol. 33, pp. 1404–1406, 1974.

[3] G. T. Bodwin, E. Braaten, E. Eichten, S. L. Olsen, T. K. Pedlar, and J. Russ, "Quarkonium at the frontiers of high energy physics: a snowmass white paper," 2013, https://arxiv.org/abs/1307.7425.

[4] N. Brambilla, S. Eidelman, B. K. Heltsley et al., "Heavy quarkonium: progress, puzzles, and opportunities," *The European Physical Journal C*, vol. 71, no. 2, p. 1534, 2011.

[5] A. Alfonso Albero, A. Camboni, S. Coquereau et al., "Near-threshold $D\bar{d}$ spectroscopy and observation of a new charmonium state," *Journal of High Energy Physics*, vol. 2019, no. 7, p. 35, 2019.

[6] M. Tanabashi, K. Hagiwara, K. Hikasa et al., "Review of particle physics," *Physical Review D*, vol. 98, article 030001, 2018.

[7] T. Barnes, S. Godfrey, and E. S. Swanson, "Higher charmonia," *Physical Review D*, vol. 72, no. 5, article 054026, 2005.

[8] S. Godfrey and N. Isgur, "Mesons in a relativized quark model with chromodynamics," *Physical Review D*, vol. 32, pp. 189–231, 1985.

[9] O. Lakhina and E. S. Swanson, "Dynamic properties of charmonium," *Physical Review D*, vol. 74, no. 1, article 014012, 2006.

[10] B.-Q. Li and K.-T. Chao, "Higher charmonia and x, y, z states with screened potential," *Physical Review D*, vol. 79, no. 9, article 094004, 2009.

[11] W. Lucha, F. F. Schöberl, and D. Gromes, "Bound states of quarks," *Physics Reports*, vol. 200, no. 4, pp. 127–240, 1991.

[12] N. Brambilla, A. Pineda, J. Soto, and A. Vairo, "Effective-field theories for heavy quarkonium," *Reviews of Modern Physics*, vol. 77, pp. 1423–1496, 2005.

[13] G. T. Bodwin, D. K. Sinclair, and S. Kim, "Quarkonium decay matrix elements from quenched lattice qcd," *Physical Review Letters*, vol. 77, pp. 2376–2379, 1996.

[14] T. Burch, C. DeTar, M. Di Pierro et al., "Quarkonium mass splittings in three-flavor lattice qcd," *Physical Review D*, vol. 81, article 034508,, 2010.

[15] C. T. H. Davies, K. Hornbostel, A. Langnau et al., "Precision Υ spectroscopy from nonrelativistic lattice qcd," *Physical Review D*, vol. 50, pp. 6963–6977, 1994.

[16] S. Piemonte, S. Collins, M. Padmanath, D. Mohler, and S. Prelovsek, "Charmonium resonances with $J^{PC} = 1^{--}$ and 3^{--} from $\bar{D}d$ scattering on the lattice," *Physical Review D*, vol. 100, article 074505, 2019.

[17] S. Bhatnagar and L. Alemu, "Approach to calculation of mass spectra and two-photon decays of$c\bar{c}$mesons in the framework of Bethe-Salpeter equation," *Physical Review D*, vol. 97, no. 3, article 034021, 2018.

[18] M. Blank and A. Krassnigg, "Bottomonium in a bethe-salpeter-equation study," *Physical Review D*, vol. 84, article 096014, 2011.

[19] T. Hilger, C. Popovici, M. Gómez-Rocha, and A. Krassnigg, "Spectra of heavy quarkonia in a bethe-salpeter-equation approach," *Physical Review D*, vol. 91, article 034013, 2015.

[20] H. Negash and S. Bhatnagar, "Mass spectrum and leptonic decay constants of ground and radially excited states of ηc and ηb in a bethe–salpeter equation framework," *International Journal of Modern Physics E*, vol. 24, no. 4, article 1550030, 2015.

[21] E. J. Eichten, K. Lane, and C. Quigg, "b-meson gateways to missing charmonium levels," *Physical review letters*, vol. 89, article 162002, 2002.

[22] E. J. Eichten and C. Quigg, "Quarkonium wave functions at the origin," *Physical Review D*, vol. 52, no. 3, p. 1726, 1995.

[23] E. Eichten, K. Gottfried, T. Kinoshita, K. D. Lane, and T. M. Yan, "Interplay of confinement and decay in the spectrum of charmonium," *Physical Review Letters*, vol. 36, pp. 500–504, 1976.

[24] E. Eichten, K. Gottfried, T. Kinoshita, K. D. Lane, and T. M. Yan, "Charmonium: the model," *Physical Review D*, vol. 17, pp. 3090–3117, 1978.

[25] E. Eichten, K. Gottfried, T. Kinoshita, K. D. Lane, and T. M. Yan, "Charmonium: comparison with experiment," *Physical Review D*, vol. 21, pp. 203–233, 1980.

[26] G. S. Bali, B. Bolder, N. Eicker et al., "Static potentials and glueball masses from qcd simulations with wilson sea quarks," *Physical Review D*, vol. 62, article 054503, 2000.

[27] G. S. Bali, "Qcd forces and heavy quark bound states," *Physics Reports*, vol. 343, no. 1-2, pp. 1–136, 2001.

[28] W. Lucha and F. F. Schöberl, "Solving the schrödinger equation for bound states with mathematica 3.0," *International Journal of Modern Physics C*, vol. 10, no. 4, pp. 607–619, 1999.

[29] S. Patel, P. C. Vinodkumar, and S. Bhatnagar, "Decay rates of charmonia within a quark-antiquark confining potential," *Chinese Physics C*, vol. 40, no. 5, article 053102, 2016.

[30] J.-L. Domenech-Garret and M.-A. Sanchis-Lozano, "Qq-onia package: a numerical solution to the schrödinger radial equation for heavy quarkonium," *Computer Physics Communications*, vol. 180, no. 5, pp. 768–778, 2009.

[31] V. Mateu, P. G. Ortega, D. R. Entem, and F. Fernández, "Calibrating the nave cornell model with nrqcd," *The European Physical Journal C*, vol. 79, no. 4, p. 323, 2019.

[32] M. Sakai, Y. Matsuda, M. Hirano, and K. Katō, "A partial width calculation of ozi-allowed charmonium decays in a coupled channel framework," *Few-Body Systems*, vol. 46, no. 3, pp. 189–198, 2009.

[33] R. Kumar and F. Chand, "Asymptotic study to the n-dimensional radial Schrödinger equation for the quark-antiquark system," *Communications in Theoretical Physics*, vol. 59, no. 5, p. 528, 2013.

[34] H. Mutuk, "Spin averaged mass spectrum of heavy quarkonium via asymptotic iteration method," *Canadian Journal of Physics*, vol. 97, no. 12, pp. 1342–1348, 2019.

[35] R. Rani, S. B. Bhardwaj, and F. Chand, "Mass spectra of heavy and light mesons using asymptotic iteration method," *Communications in Theoretical Physics*, vol. 70, no. 2, p. 179, 2018.

[36] F. Brau and C. Semay, "The three-dimensional Fourier grid Hamiltonian method," *Journal of computational physics*, vol. 139, no. 1, pp. 127–136, 1998.

[37] K. V. Kumar and A. P. Monteiro, "Heavy quarkonium spectra and its decays in a nonrelativistic model with Hulthen potential," *Journal of Physics G: Nuclear and Particle Physics*, vol. 38, no. 8, article 085001, 2011.

[38] S. F. Radford and W. W. Repko, "Potential model calculations and predictions for heavy quarkonium," *Physical Review D*, vol. 75, article 074031, 2007.

[39] D. T. Colbert and W. H. Miller, "A novel discrete variable representation for quantum mechanical reactive scattering via the s-matrix kohn method," *The Journal of chemical physics*, vol. 96, no. 3, pp. 1982–1991, 1992.

[40] D. O. Harris, G. G. Engerholm, and W. D. Gwinn, "Calculation of matrix elements for one-dimensional quantum-mechanical problems and the application to anharmonic oscillators," *The*

Journal of Chemical Physics, vol. 43, no. 5, pp. 1515–1517, 1965.

[41] Z. Bačić and J. C. Light, "Highly excited vibrational levels of "floppy" triatomic molecules: a discrete variable representation–distributed Gaussian basis approach," *Journal of chemical physics*, vol. 85, no. 8, pp. 4594–4604, 1986.

[42] Z. Bačić and J. C. Light, "Accurate localized and delocalized vibrational states of hcn/hnc," *Journal of chemical physics*, vol. 86, no. 6, pp. 3065–3077, 1987.

[43] S. E. Choi and J. C. Light, "Determination of the bound and quasibound states of ar–hcl van der Waals complex: discrete variable representation method," *The Journal of Chemical Physics*, vol. 92, no. 4, pp. 2129–2145, 1990.

[44] J. C. Light, I. P. Hamilton, and J. V. Lill, "Generalized discrete variable approximation in quantum mechanics," *The Journal of Chemical Physics*, vol. 82, no. 3, pp. 1400–1409, 1985.

[45] J. V. Lill, G. A. Parker, and J. C. Light, "Discrete variable representations and sudden models in quantum scattering theory," *Chemical Physics Letters*, vol. 89, no. 6, pp. 483–489, 1982.

[46] R. M. Whitnell and J. C. Light, "Efficient pointwise representations for vibrational wave functions: eigenfunctions of h+3," *The Journal of Chemical Physics*, vol. 90, no. 3, pp. 1774–1786, 1989.

[47] L. Bytautas, N. Matsunaga, T. Nagata, M. S. Gordon, and K. Ruedenberg, "Accurate ab initio potential energy curve of f 2. iii. the vibration rotation spectrum," *The Journal of chemical physics*, vol. 127, no. 20, article 204313, 2007.

[48] M. Chrysos, O. Gaye, and Y. Le Duff, "Quantum analysis of absolute collision-induced scattering spectra from bound, metastable and free ar diatoms," *The Journal of chemical physics*, vol. 105, no. 1, pp. 31–36, 1996.

[49] P. Fassbinder and W. Schweizer, "Hydrogen atom in very strong magnetic and electric fields," *Physical Review A*, vol. 53, pp. 2135–2139, 1996.

[50] J. Komasa, M. Puchalski, P. Czachorowski, G. Łach, and K. Pachucki, "Rovibrational energy levels of the hydrogen molecule through nonadiabatic perturbation theory," *Physical Review A*, vol. 100, article 032519, 2019.

[51] Y. Liu, W. Hu, S. Luo et al., "Vibrationally resolved above-threshold ionization in no molecules by intense ultrafast two-color laser pulses: an experimental and theoretical study," *Physical Review A*, vol. 100, article 023404, 2019.

[52] V. S. Melezhik, "Three-dimensional hydrogen atom in crossed magnetic and electric fields," *Physical Review A*, vol. 48, pp. 4528–4538, 1993.

[53] G. A. Pitsevich and A. E. Malevich, "Comparison of the Fourier and discrete-variable-representation methods in the numerical solution of multidimensional Schrödinger equations," *Journal of Applied Spectroscopy*, vol. 82, no. 6, pp. 893–900, 2016.

[54] H. Salami, T. Bergeman, B. Beser et al., "Spectroscopic observations, spin-orbit functions, and coupled-channel deperturbation analysis of data on the $a^1\Sigma_u^+$ and $b^3\Pi_u$ states of rb_2," *Physical Review A*, vol. 80, article 022515, 2009.

[55] W. Schweizer and P. Fassbinder, "Discrete variable method for nonintegrable quantum systems," *Computers in Physics*, vol. 11, no. 6, pp. 641–646, 1997.

[56] T. Seideman and W. H. Miller, "Calculation of the cumulative reaction probability via a discrete variable representation with absorbing boundary conditions," *The Journal of Chemical Physics*, vol. 96, no. 6, pp. 4412–4422, 1992.

[57] J. C. Light and T. Carrington Jr., "Discrete-variable representations and their utilization," *Advances in Chemical Physics*, vol. 114, pp. 263–310, 2000.

[58] W. Schweizer, "Discrete variable method: numerical quantum dynamics," in *Progress in Theoretical Chemistry and Physics*, vol. 9, Springer, Dordrecht, 2002.

[59] V. Kher and A. K. Rai, "Spectroscopy and decay properties of charmonium," *Chinese Physics C*, vol. 42, no. 8, article 083101, 2018.

[60] N. R. Soni, B. R. Joshi, R. P. Shah, H. R. Chauhan, and J. N. Pandya, "Spectroscopy using the Cornell potential," *The European Physical Journal C*, vol. 78, no. 7, p. 592, 2018.

[61] M. Atif Sultan, N. Akbar, B. Masud, and F. Akram, "Higher hybrid charmonia in an extended potential model," *Physical Review D*, vol. 90, article 054001, 2014.

[62] V. R. Debastiani and F. S. Navarra, "A non-relativistic model for the $[cc][\bar{c}\bar{c}]$ tetraquark," *Chinese Physics C*, vol. 43, no. 1, article 013105, 2019.

[63] W. Kwong, P. B. Mackenzie, R. Rosenfeld, and J. L. Rosner, "Quarkonium annihilation rates," *Physical Review D*, vol. 37, pp. 3210–3215, 1988.

[64] R. Van Royen and V. F. Weisskopf, "Hardon decay processes and the quark model," *Il Nuovo Cimento A (1971-1996)*, vol. 50, no. 3, pp. 617–645, 1967.

[65] N. Akbar, "Decay properties of conventional and hybrid charmonium mesons," *Journal of the Korean Physical Society*, vol. 77, no. 1, pp. 17–24, 2020.

[66] W.-J. Deng, H. Liu, L.-C. Gui, and X.-H. Zhong, "Charmonium spectrum and their electromagnetic transitions with higher multipole contributions," *Physical Review D*, vol. 95, no. 3, article 034026, 2017.